

Article

Degradation of Reinforced Concrete Beams Subjected to Sustained Loading and Multi-Environmental Factors

Shengyuan Li ^{1,2} , Henglin Lv ^{1,2,*}, Tianhua Huang ¹, Zhigang Zhang ¹, Jin Yao ¹ and Xin Ni ¹

¹ School of Mechanics and Civil Engineering, China University of Mining and Technology, Xuzhou 221116, China

² Jiangsu Collaborative Innovation Center of Building Energy Saving and Construction Technology, Jiangsu Vocational Institute of Architectural Technology, Xuzhou 221116, China

* Correspondence: henglinlv@cumt.edu.cn

Abstract: In the process of service, reinforced concrete structures have to bear both load and multi-environmental factors. The deterioration of reinforced concrete beams is critical to the durability, safety, and sustainability of reinforced concrete structures. The main aim of the present research is to determine the degradation mechanism of reinforced concrete beams subjected to sustained loading and multi-environmental factors. Reinforced concrete beam specimens were prepared, loaded and then exerted multi-environmental factors. At the end of each degradation period, the degradation of concrete (chemical contents of concrete beam surfaces, carbonation depth, compressive strength and maximum cracks) and the corrosion of steel bars (corrosion ratio and tensile strength) were continuously measured. Moreover, degraded reinforced concrete beams were flexural loaded in four-point bending failure tests. The degradation mechanism of reinforced concrete beams subjected to sustained loading and multi-environmental factors was analyzed. Thus, this study can promote a comprehensive understanding of reinforced concrete beams subjected to sustained loading and multi-environmental factors.

Keywords: reinforced concrete beams; degradation; sustained loading; multi-environmental factors



Citation: Li, S.; Lv, H.; Huang, T.; Zhang, Z.; Yao, J.; Ni, X. Degradation of Reinforced Concrete Beams Subjected to Sustained Loading and Multi-Environmental Factors. *Buildings* **2022**, *12*, 1382. <https://doi.org/10.3390/buildings12091382>

Academic Editors: Youde Wang, Baiqiao Chen, Liang Zong and Zongxing Zhang

Received: 5 August 2022

Accepted: 31 August 2022

Published: 5 September 2022

Publisher's Note: MDPI stays neutral with regard to jurisdictional claims in published maps and institutional affiliations.



Copyright: © 2022 by the authors. Licensee MDPI, Basel, Switzerland. This article is an open access article distributed under the terms and conditions of the Creative Commons Attribution (CC BY) license (<https://creativecommons.org/licenses/by/4.0/>).

1. Introduction

Due to its versatility and relatively low cost, concrete has turned into the most widely used man-made material and preferred material for civil engineering and infrastructure construction in environmental factors. As the main bearing members of concrete structures, reinforced concrete beams have to bear loads in the process of actual service. Moreover, reinforced concrete beams also suffer environmental factors attack, such as acid, salt, temperature and periodic changes of temperature and humidity [1,2].

Concrete performance is associated with the characteristics of the raw material, including cement types [3] and aggregate [4]. When chloride ions migrate into cementitious concrete through diffusion, wicking and absorption, they cause complex chemical reactions with cementitious concrete in environmental factors. [5,6]. In the migration process of chloride ions, a specific proportion of chloride ions are bound by the cement matrix, and some free chloride ions are preserved in pore solution [2,7]. Moreover, sulphate also causes the deterioration of cementitious concrete in concrete structures [8–11]. In ordinary Portland cement, Portlandite leads to the deterioration of concrete in sulphate environment, because it is the hydration product most susceptible to sulphate attack. [12]. Because of the constitutive relation change of degraded concrete, the mechanical properties of reinforced concrete beams are decreased [13,14]. Usually, the presentation of deteriorated concrete is the change of carbonation depth [15–18], compressive strength [19,20], and so on [21,22].

In corrosion environment, chloride ions and sulfates react with cementitious material, which reduces basicity of concrete and destroys passivation film on surface of steel rebar [23]. Then, chloride ion is absorbed on surface layer of steel rebar, and steel rebar

starts to corrode because of the chloride ions. More severely, sufficient oxygen and moisture accelerates corrosion rate [24]. With corrosion occurrence, the expanded volume of the corrosion product is about two to six times the original volume. Volume expansion will produce increasing extensive pressure on the interface between the steel rebar and concrete [25]. Moreover, volume expansion after steel corrosion will lead to cracking along steel rebar, surface delamination, the spalling of concrete, the loss of the adhesion between steel and concrete and the decrease of the transverse-sectional area of a reinforced concrete beam [26,27].

For the reinforced concrete beam, the strength [28,29], stiffness, ductility [30] and energy consumption capacity [31] are decreased with the sustained aging and deterioration through environmental factors during its service life. Some researchers have investigated the capacity decrease of deteriorated reinforced concrete beams in a marine environment [32–36]. In the initial stage, the flexural strength of a reinforced concrete beam is not significantly affected by the corrosion of longitudinal reinforcement. In contrast, stiffness and flexural strength are remarkably reduced, owing to a deficit of the longitudinal section [13,14].

In a previous study, a coal mine's condition was given by specifying the parameters of acid–salt mist, carbon dioxide and temperature and humidity. Based on this, the deterioration behavior of reinforced concrete beam was presented [1] and the degradation model of bond performance between deteriorated concrete and corroded deformed steel bars was proposed [37]. However, the coal mine condition in existing research simply simulates environmental factors and lacks the loading condition.

The main contribution in this work is the combined use of sustained loading and multi-environmental factors: acid–salt mist, carbon dioxide and the periodic change of temperature and humidity. The effect of each of these factors has been previously investigated but only when acting independently. In this study, the concrete deterioration, steel corrosion and flexural performance of deteriorated reinforced concrete beams subjected to sustained loading and multi-environmental factors are further studied. First, reinforced concrete beam specimens are made and the interaction action of sustained loading and multi-environmental factors on the reinforced concrete beam specimens are introduced in Section 2. In Section 3, concrete deterioration, steel corrosion and flexural performance of deteriorated reinforced concrete beams are presented, and the deterioration mechanism of reinforced concrete beams subjected to sustained loading and multi-environmental factors is discussed. Section 4 concludes the paper.

2. Experimental Program

2.1. Materials

In our study, Portland cement with a 2.5% loss on ignition is adopted to make beam specimens. Table 1 lists the chemical composition of the cementitious material. Gravels with sizes 5–31.5 mm were used as coarse aggregate. River sand with a fineness modulus of 2.9 and the maximum size of 9.5 mm was used as fine aggregate. The laboratory tap water was used. Table 2 gives the mix proportion of concrete used in this study.

Table 1. Chemical composition of cementitious material (% by mass).

Chemical Composition	SiO ₂	Al ₂ O ₃	Fe ₂ O ₃	CaO	MgO	SO ₃
Content (%)	21.5	5.61	3.27	53.9	3.3	2.3

Table 2. Mix proportion of concrete.

Water (kg/m ³)	Cement (kg/m ³)	Sand (kg/m ³)	Gravel (kg/m ³)
325	195	762	1144

2.2. Beam Specimen

The beam specimens used in this experiment are 2 m long double-reinforced rectangular reinforced concrete beams with the cross-sectional dimension of 200 mm × 400 mm (width × height). Figure 1 shows beam specimen configuration from side and cross-sectional views. Two ribbed bars with the diameter of 14 mm were placed on the top of the beam as hangers. Two ribbed bars with an 18 mm diameter and one ribbed bars with a 16 mm diameter were placed on the bottom of the beams as a tensile rebar. Round bars with an 8 mm diameter were used as stirrups, and the stirrup spacing was 100 mm and 150 mm in the encrypted zone and the unencrypted zone, respectively.

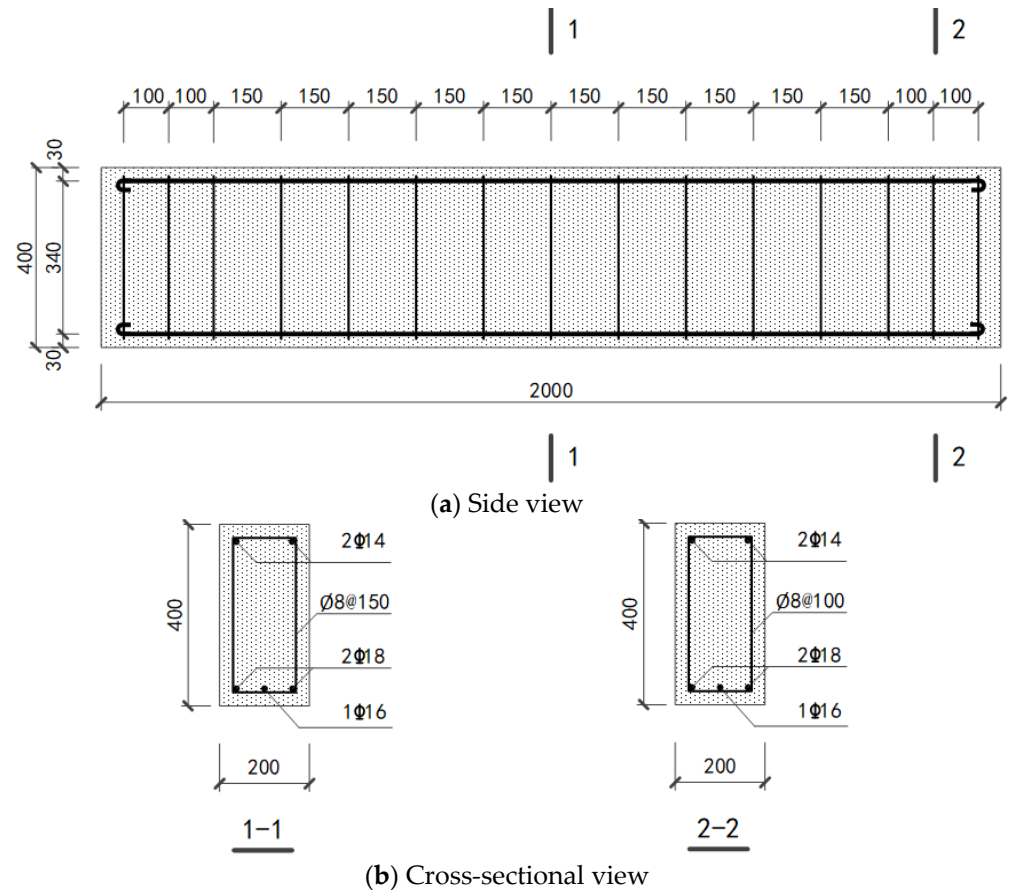


Figure 1. Beam specimen configuration from (a) side and (b) cross-sectional views (unit: mm).

A total of 22 beam specimens were made for the implemented degradation experiment. The degradation of the reinforced concrete beams was tested after each degradation period, and a total of 10 degradation periods were set. In each test, 2 beam specimens were adopted. As control group, the test data of 2 beam specimens without degradation were collected as degradation period zero.

2.3. Accelerated Deterioration Experiment of Reinforced Concrete Beams Subjected to Sustained Loading and Multi-Environmental Factors

In our study, environment parameters used to simulate multi-environmental factors were derived from coal mines in Xuzhou City, Jiangsu Province, in China. Since 2003, we have monitored temperature and humidity from several coal mines in Xuzhou. In the coal mines, corrosive substance exists in the form of gas and liquid. For the gas corrosive substance, CO_2 concentration is set at $27,692 \text{ mm}^3/\text{m}^3$ in our accelerated experiment, according to GB/T50082-2009 in China. For the liquid corrosive substance, acidic corrosive substance HCl, Cl_2 , H_2S , SO_2 and NO_x in the coal mines were converted into HCl acid mist with a concentration of $157.2 \text{ mg}/\text{m}^3$. Saline corrosive substance included NaCl,

MgCl₂ and Na₂SO₄ in the coal mines. They were set as NaCl, MgCl₂ and Na₂SO₄ salt mist with concentrations of 0.814 g/L, 9.95 g/L and 37.88 g/L, respectively. Table 3 lists the experiment parameters of the acid–salt mist, carbon dioxide and periodic change of temperature and humidity. The duration of each experiment period was set to 56 days.

Table 3. Experiment parameters of acid–salt mist, carbon dioxide and periodic change of temperature and humidity.

NaCl (g/L)	MgCl ₂ (g/L)	Na ₂ SO ₄ (g/L)	CO ₂ (mg/m ³)	HCl (mg/m ³)	Temperature/°C	Relative Humidity/%
0.814	9.95	37.88	27,692	157.2	15	80
					26	95
					15	80
					2	10

Simulation equipment of loads and environment was used to implement the accelerated deterioration experiment of reinforced concrete beams in our study. Figure 2 shows the experiment setup of the accelerated deterioration experiment of reinforced concrete beams subjected to sustained loading and multi-environmental factors. After the reinforced concrete beam specimens were placed into the simulation equipment according to the way shown in Figure 2, two symmetrical concentrated forces were applied to beams using a steel spreader beam connected with a stainless steel dowel bar and an electro-hydraulic jack in the simulation equipment. The forces were increased until the designated value. Then, mixed acid and salt fog were sprayed into the environment equipment, and the temperature and humidity were adjusted regularly according to the parameters listed in Table 3.

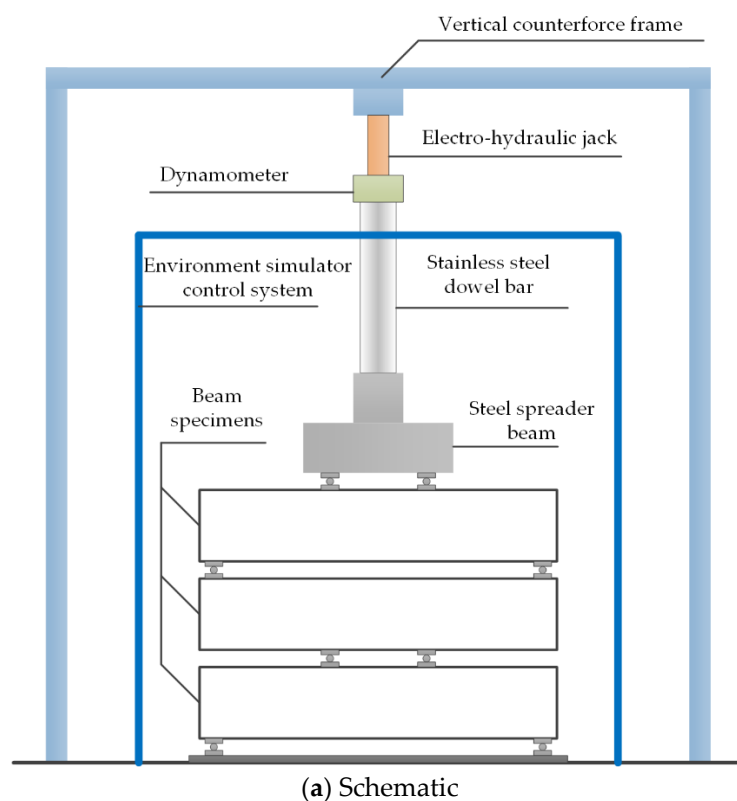


Figure 2. Cont.



(b) Real setup

Figure 2. Experiment setup of accelerated deterioration experiment of reinforced concrete beams subjected to sustained loading and multi-environmental factors: (a) schematic and (b) real setup.

3. Experimental Results and Mechanism Discussion

The performance degradation of the reinforced concrete beams due to extremely complex corrosive factors of the acid–salt mist, carbon dioxides and the periodic change of temperature and humidity. By simulating the sustained loading and multi-environmental factors, the concrete and steel bars of reinforced concrete beams in 0–10 periods are measured. This section presents the degradation of concrete, the corrosion of steel bars and the flexural performance of degraded reinforced concrete beams. Moreover, the performance degradation mechanisms of concrete, steel bars and beams are discussed.

3.1. Degradation of Concrete

At the end of each degradation period, the concrete on the degraded beam surface was ground into powders with 74 μm or less size. The chemical contents of concrete beam surfaces were measured using dried powders according to X-ray fluorescence. Moreover, two concrete core samples with 100 mm diameter and 200 mm height were drilled at the end area of the degraded beam specimen. According to the Chinese standard GB/T50344-2004, the carbonation depth of concrete was measured by spraying 1% alcohol phenolphthalein solution around the surface of a concrete core sample. Another core sample was made into a specimen with a 100 mm diameter and 100 mm height. According to the Chinese standard JGJ/T384-2016, the uniaxial compression method was adopted to measure the remaining compressive strength of the degraded concrete. In addition, the maximum crack widths on degraded reinforced concrete beams were manually measured.

3.1.1. Chemical Contents of Concrete Beam Surfaces

In the chemical contents on concrete beam surfaces, CaO was main component of cementitious material, and its decrease indicates the degradation of concrete. HCl and NaSO₄ are major aggressive factors of concrete in our experiment. Therefore, the changes of CaO, Cl and S can reflect the degradation of concrete and the accumulation of aggressive factors on concrete surfaces. The major chemical reactions during the degradation processes in which CaO is consumed by HCl and NaSO₄ are listed as follows:



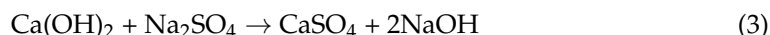
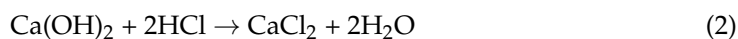


Figure 3 shows the changes of CaO, Cl and S on degraded concrete beam surfaces in 0–10 degradation periods, where the Cl and S represent the compounds related to them. With the increase of deterioration time, the contents of Cl and S on the beam surface increase significantly, while the content of CaO decreases gradually. The phenomenon means that the CaO is gradually consumed. It should be noted that the CaO in coarse aggregate could cause inaccuracies in the results of Figure 3. However, the total content of CaO (included in cement and coarse aggregate) falls with the increase of degradation period, and even the CaO in coarse aggregate is taken into account. In the 0–3 deterioration periods, the contents of Cl and S as a corrosive medium were close to zero, because there is no accumulation of Cl and S on concrete beam surfaces due to fewer degradation periods. Correspondingly, the content of CaO was nearly constant, because no chemical reaction had taken place between concrete and aggressive factors. In the 4–10 deterioration periods, CaO reacted with aggressive factors, resulting in a rapid decline in its content, because the CaCl_2 dissolved in the water and decreased as the sand rises. With the CaSO_4 accumulating continuously, a diaphragm was formed on concrete surfaces, which decreases the reaction rate of aggressive factors with a concrete inside of beams. The diaphragm intercepted the aggressive factors. As a result, decline rate of CaO slows down after eight deterioration periods, and the contents of Cl and S on concrete beam surfaces increase.

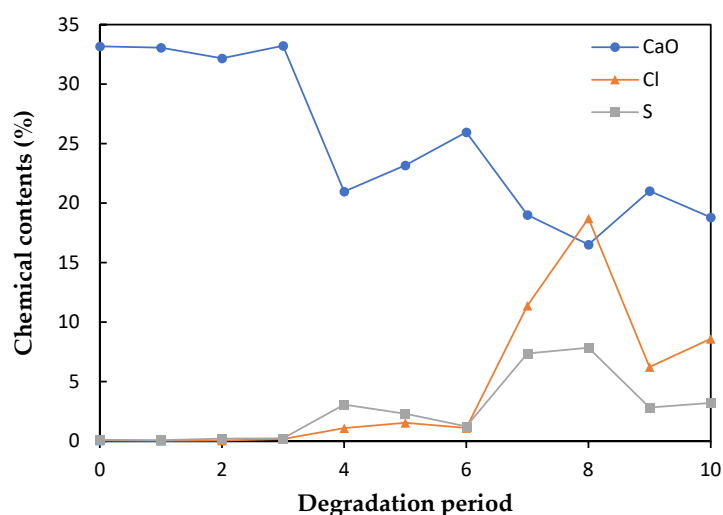


Figure 3. CaO, Cl and S on degraded concrete beam surfaces in 0–10 degradation periods.

3.1.2. Carbonation Depth

When exposed to environmental factors, CO_2 will carbonize concrete. The carbonation of concrete reduces durability. The major chemical carbonation reactions of concrete, in which CaCO_3 is formed, are presented in Equations (4) and (5). In acid–salt mist, carbon dioxide and the periodic change of temperature and humidity in the environment, HCl dissolves CaCO_3 . The chemical dissolution reaction is shown in Equation (6).

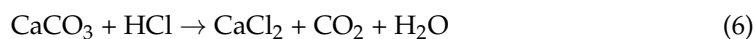
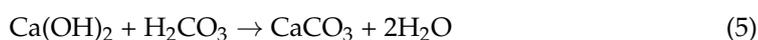


Figure 4 presents a concrete core sample sprayed with 1% alcohol phenolphthalein solution for carbonation depth measurement. The junction of discoloration and non-discoloration is defined as the interface of concrete carbonation. A vernier caliper is used to measure

the vertical distance from the interface to the concrete surface multiple times, and the average value is the carbonation depth value of deteriorated concrete. Figure 5 shows the carbonation depth of degraded concrete in 0–10 degradation periods. It can be observed that carbonation depth increases with deterioration period. In the process of carbonation, CaCO_3 is produced contiguously. At the initial stage of carbonation, CaCO_3 blocks the internal pores of concrete. Then, the internal pores are broken by excess CaCO_3 , which opens routes for CO_2 to invade. As a result, the opened routes in turn accelerate the carbonation of concrete. Moreover, HCl dissolves CaCO_3 and opens concrete pores, which also promoted carbonation in the concrete. In addition, cracks and spalls also accelerate the carbonation of concrete. When the carbonation depth is equal to the thickness of the concrete protective layer, it will lead to the corrosion of steel bars.



Figure 4. Concrete core sample sprayed with 1% alcohol phenolphthalein solution to measure carbonation depth.

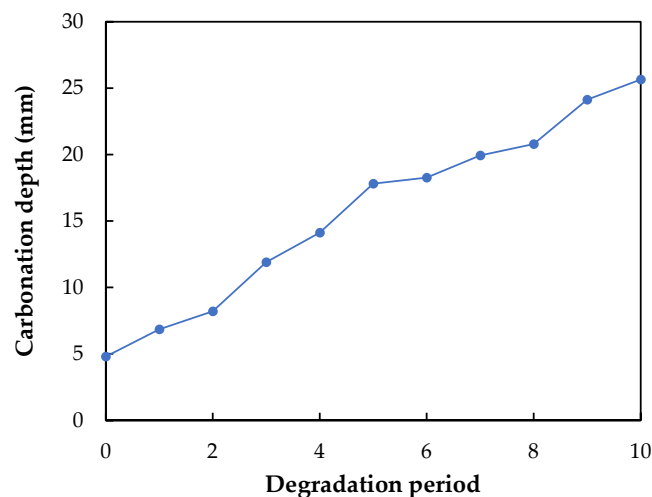


Figure 5. Carbonation of degraded concrete in 0–10 degradation periods.

3.1.3. Compressive Strength

The compressive strength of concrete directly affects mechanical properties of reinforced concrete beams. Therefore, to measure the compressive strength of concrete, we drilled two concrete core samples at the end area of the degraded reinforced concrete beams after each degradation period. The compressive strengths of the two concrete core samples were computed as compressive strength in each degradation period.

The average compressive strengths of concrete core samples in 0–10 degradation periods are presented in Figure 6. The compressive strengths of concrete core samples increased first and then decreased with the increase of deterioration periods. At the initial stage of carbonation, the concrete was dense because the CaCO_3 blocked the internal pores of concrete. The compacted concrete causes a slight increase in compressive strength in

1st–3rd degradation periods. With degradation intensifying, the internal pores of concrete were broken by accumulated CaCO_3 , which makes the concrete loose. As a result, the compressive strengths of concrete reduced constantly in 4th–10th degradation periods.

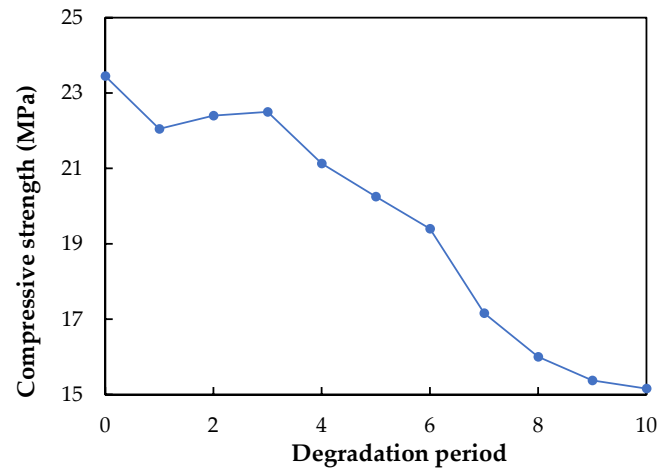


Figure 6. Compressive strengths of concrete core samples in 0–10 degradation periods.

3.1.4. Maximum Crack Width

Cracks are typical indicator of reinforced concrete beam deformation, and they can visually reflect the decrease of the bearing capacity, durability and waterproofness of reinforced concrete beams. Under sustained loading and multi-environmental factors, the maximum crack widths of degraded reinforced concrete beams are measured after each degradation period.

Figure 7 shows maximum crack widths measured on the surface of degraded reinforced concrete beams in the degradation periods 0–10. The maximum crack widths increase slowly in exponential form in the degradation periods 0–10. There is an uncompact interface area at the interface between reinforcement and concrete, which provides space for the accumulation of corrosion products. Therefore, in the degradation periods 0–3, although rebar corrosion occurred, there was no increase of maximum crack width. After the interface area is filled, micro cracks in concrete provide routes for aggressive factors, which accelerate the corrosion of steel bars. As a result, maximum concrete crack widths increased rapidly in the degradation periods 4–10.

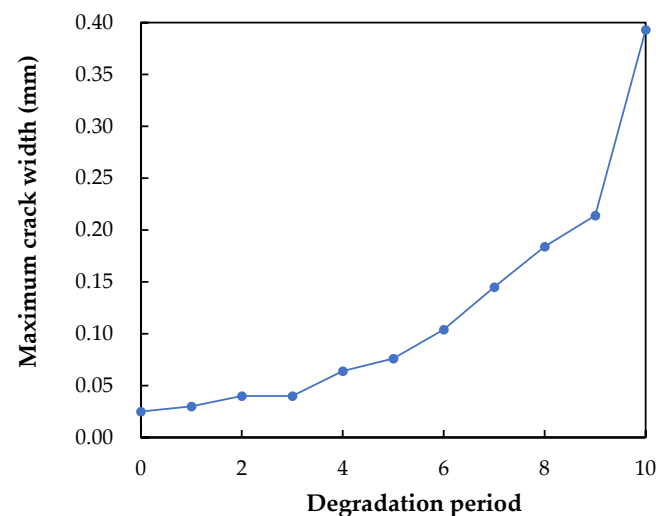


Figure 7. Maximum crack widths measured on the surface of degraded reinforced concrete beams in the degradation periods 0–10.

3.2. Corrosion of Steel Bars

During the hydration of cement, $\text{Ca}(\text{OH})_2$ is produced and dissolved in internal pores of concrete, which provide an alkaline environment for steel bars. In the alkaline environment, a passivation film covers the surface of steel bars. In our experimental environment, there were a lot of Cl ions and H ions. Due to their small particle size and high activity, they easily entered the interior of reinforced concrete beams and reacted with the $\text{Ca}(\text{OH})_2$ in concrete pores. With the decrease of PH value in concrete pores, the passivation film on surface of steel bars is destroyed and then corrosion of steel bars occurs. In the acid–salt mist, carbon dioxide and the periodic change of temperature and humidity in the environment, HCl acid mist accelerates the decrease of PH value in concrete pores. Moreover, sustained loading produces cracks in the internal concrete structure, which provides transmission routes for HCl and aggravates the corrosion of steel bars.

At the end of each degradation period, two degraded beam specimens are broken to take corroded steel bars out. Figure 8 shows some corroded steel bars of degraded reinforced concrete beams. Before measuring the corrosion rate, refrain steel bars and stirrups were preserved in a dry environment to prevent them from being corroded by the surrounding environment. The corroded steel bars are cleaned by hydrochloric acid, and then polished and dried to measure the corrosion rate according to weight loss. The two ends of the longitudinal steel bars were cut off for the tensile test, as shown in Figure 8b. The yield strength and ultimate strength of the corroded steel bars were measured. To reduce inaccurate measurements, the corrosion rate and strength were tested as fast as possible.

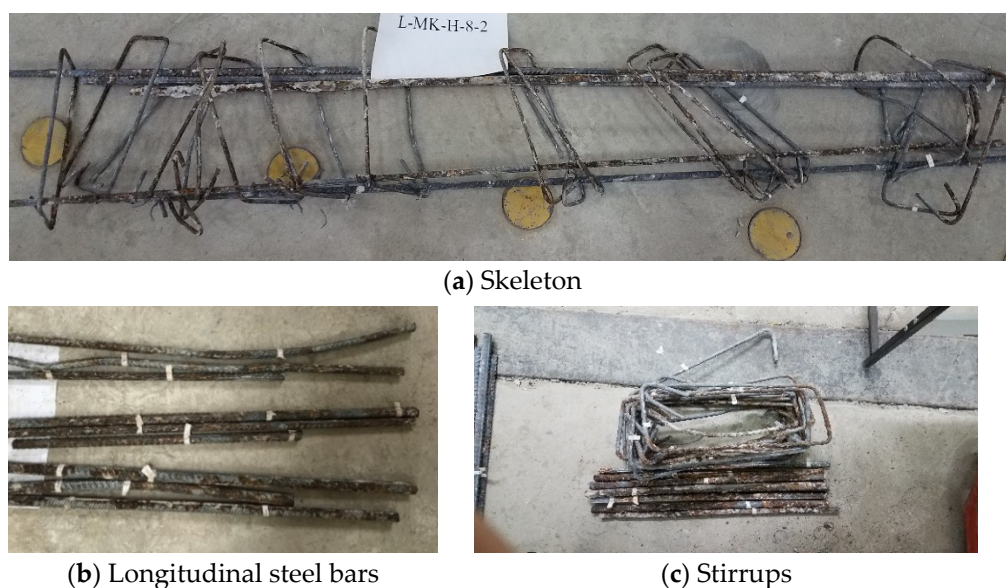


Figure 8. Corroded steel bars from degraded reinforced concrete beams: (a) skeleton, (b) longitudinal steel bars and (c) stirrups.

3.2.1. Corrosion Rate

Corrosion of steel bar makes the cross section of steel bar smaller, which reduces the strength of steel bar. In addition, the accumulation of the steel corrosion products produces the expansion force that causes concrete cracking, which reduces the bond between steel and concrete.

Figure 9 shows the average corrosion rate of stirrups and longitudinal steel bars with original diameters of 14, 16 and 18 mm in the degradation periods 0–10. It was found that corrosion rates of the steel bars were about zero in the first degradation period but increased almost linearly in the degradation periods 1–10. Moreover, because stirrups are more easily exposed to erosive substances, stirrups corrode more severely than longitudinal steel bars. In addition, tension bars (longitudinal steel bars with original diameters of 16 mm and 18 mm) corroded more severely than compression bars (longitudinal steel bars with original

diameter of 14 mm), because beams create cracks at the bottom, which provide passages for aggressive factors to enter. For the tension bars with original diameters of 16 mm and 18 mm, the corrosion rates of steel bars with original diameters of 18 mm were slightly larger. The possible reason for this phenomenon is that concrete is usually damaged by sulfate erosion at edges, and the edges of beams are easily damaged during transportation.

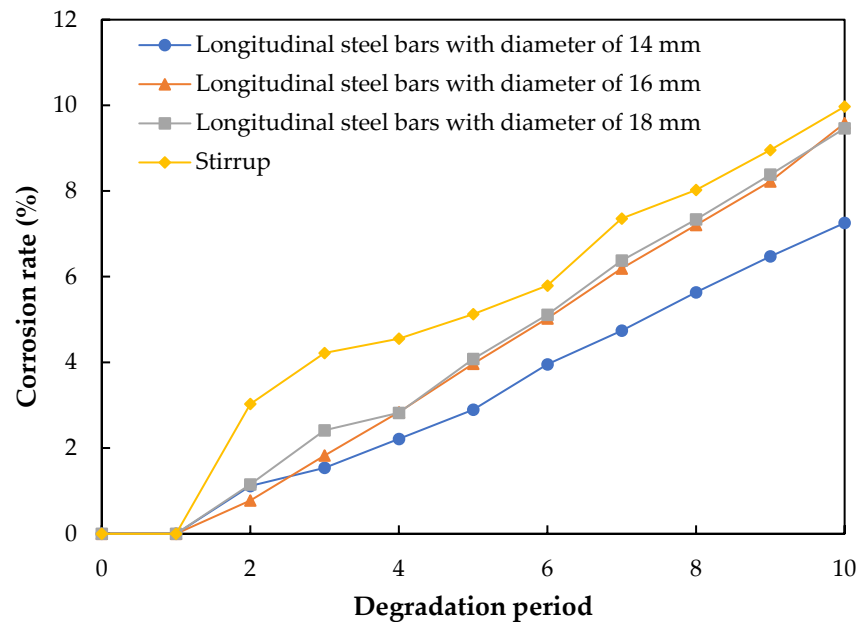


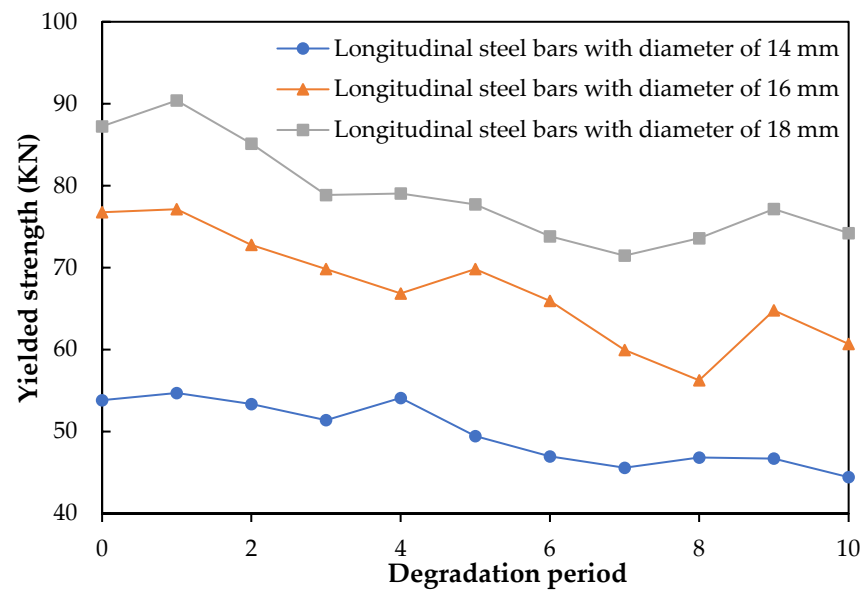
Figure 9. Average corrosion rate of stirrups and longitudinal steel bars with diameters of 14, 16 and 18 mm in the degradation periods 0–10.

3.2.2. Tensile Strength

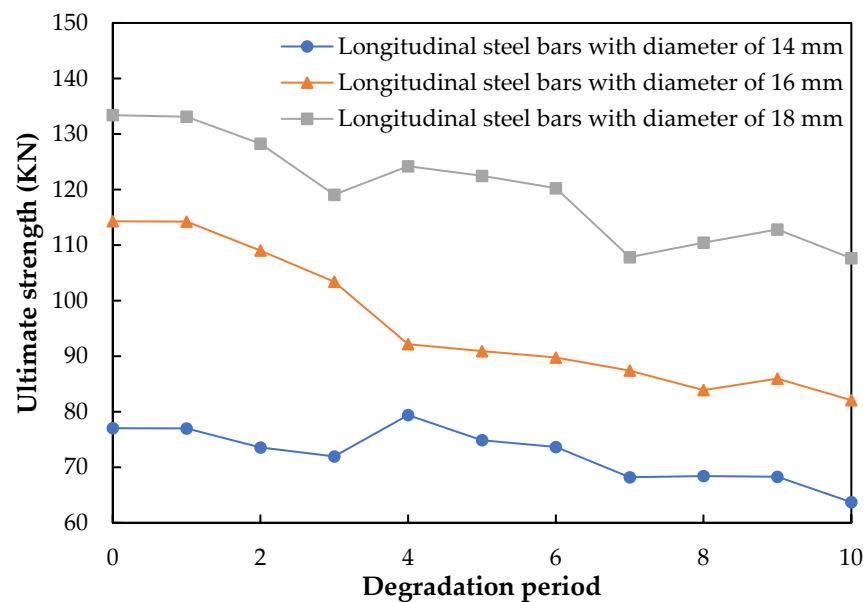
Corrosion reduces the tensile strength of steel bars, which decreases the bearing capacity of reinforced concrete beams. Figure 10 shows tensile test experiment of corroded longitudinal steel bars according to the Chinese standard GB/T228.1-2010. Figures 11a,b, respectively, show the changes of the average yielded strengths and the ultimate strengths of corroded longitudinal steel bars with diameters of 14, 16 and 18 mm. In the first degradation period, yielded strengths and ultimate strengths show little change compared with the initial stage. The phenomenon is matched with the change of corrosion rate in Figure 9, where the corrosion rates were about zero during the first degradation period. In the degradation periods 1–10, the tensile strengths of steel bars show a downward trend on the whole, because the gradually increased corrosion rates reduce the cross-sectional areas of steel bars with the increase of the degradation periods.



Figure 10. Tensile test experiment of corroded longitudinal steel bars.



(a) Yielded strengths



(b) Ultimate strengths

Figure 11. Tensile strengths of corroded longitudinal steel bars: (a) average yielded strengths and (b) average ultimate strengths.

3.3. Flexural Performance of Degraded and Reinforced Concrete Beams

The deterioration of concrete and steel bars affects the performance of beams. To check the flexural performance of degraded reinforced concrete beams, load-deflection curves are measured.

To measure the flexural performance of degraded reinforced concrete beams, four-point bending failure tests were implemented. Figure 12 shows the four-point bending failure test setup of degraded reinforced concrete beams. A steel spreader beam was used to transfer load from a hydraulic jack. Three linear variable displacement transducers were located at the mid-span supports. The reinforced concrete beams were loaded with two point loads spaced at 500 mm. The distance between the point load and the support was 650 mm, while the beam extended 100 mm from the support.

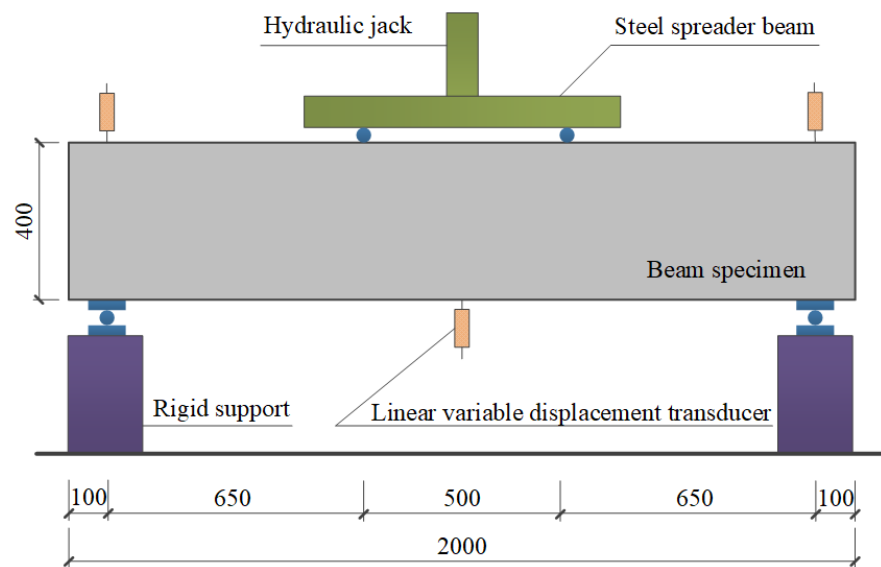


Figure 12. Four-point bending failure test setup of degraded, reinforced concrete beams (unit: mm).

According to the four-point bending failure test results, load versus mid-span deflection curves in the mid-span of degraded reinforced concrete beams in the degradation periods 0–10 are drawn in Figure 13. In the approximate elastic stage, the slopes of load–deflection curves gradually increase with the degradation periods. It should be noted that the load–deflection curve of the 6th degradation period does not show a yield point of degraded, reinforced concrete beams compared with other curves. The reason may be that the linear variable displacement transducers loosen in the four-point bending failure test.

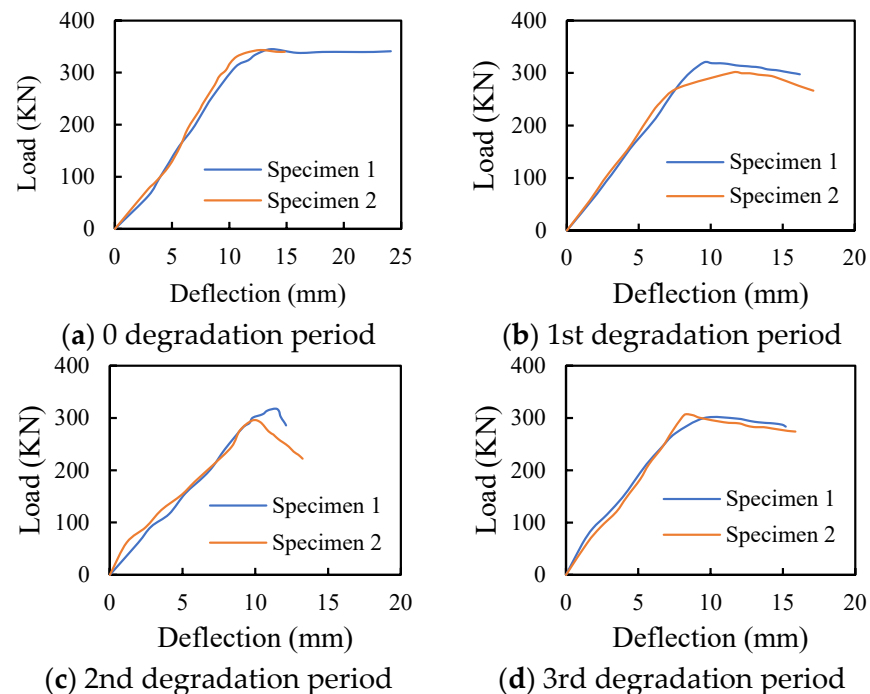


Figure 13. Cont.

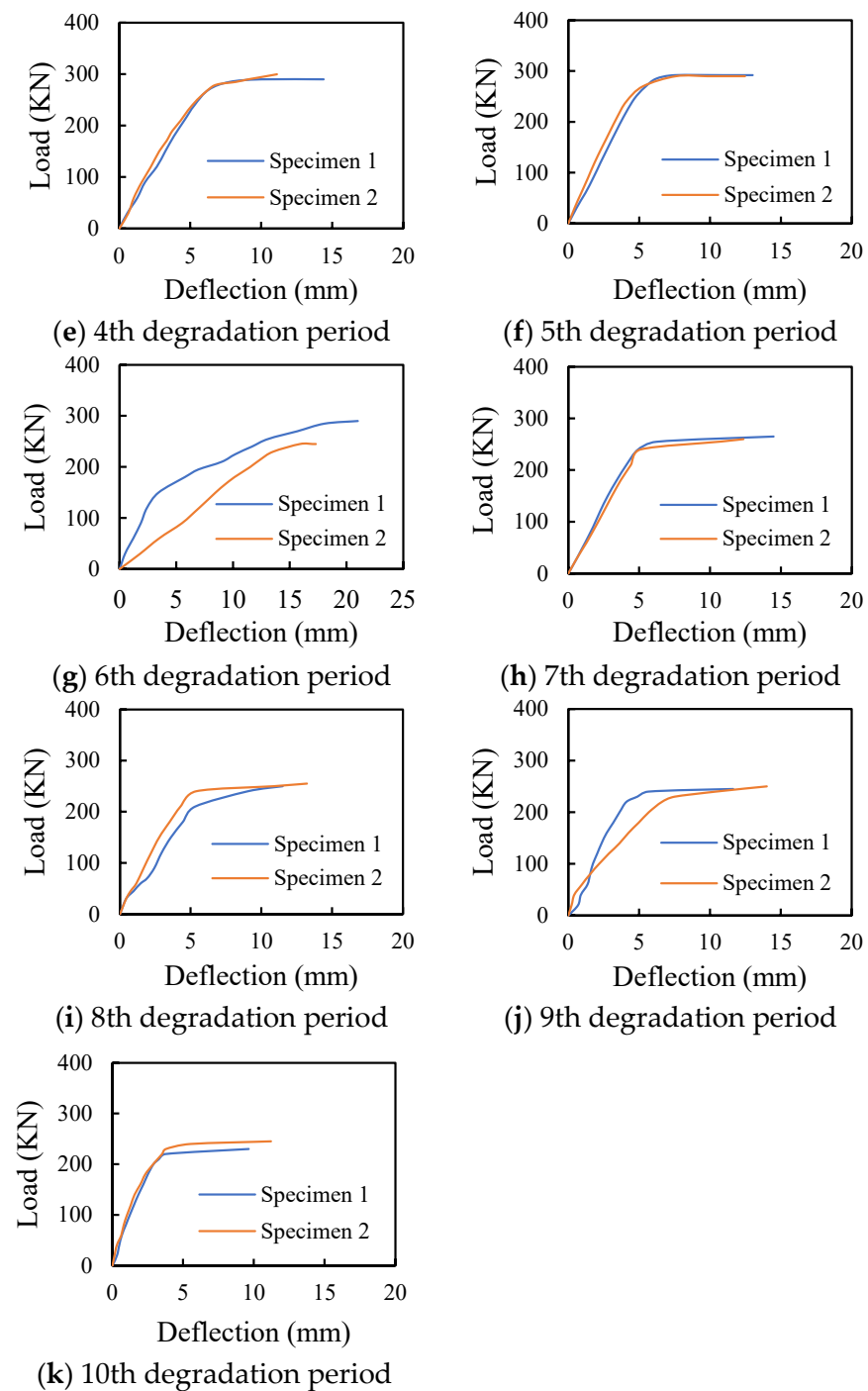


Figure 13. Load versus mid-span deflection relationship in the degradation periods 0–10: (a) 0 degradation period to (k) 10th degradation period.

Figure 14 records the ultimate loads of the degraded reinforced concrete beams in the degradation periods 0–10. The ultimate loads of the degraded reinforced concrete beams descend gradually throughout the degradation periods. As the degradation periods increasing, the performance of concrete and steel bars is weakened. As a result, the ultimate loads of degraded reinforced concrete beams descend gradually. The decrease of concrete's compressive strength and steel bars' tensile strength is the main cause of the loss of ultimate loads. Moreover, the cracks on beam surfaces resulting from sustained loading provide routes for aggressive factors, which promotes the degradation processes of beams.

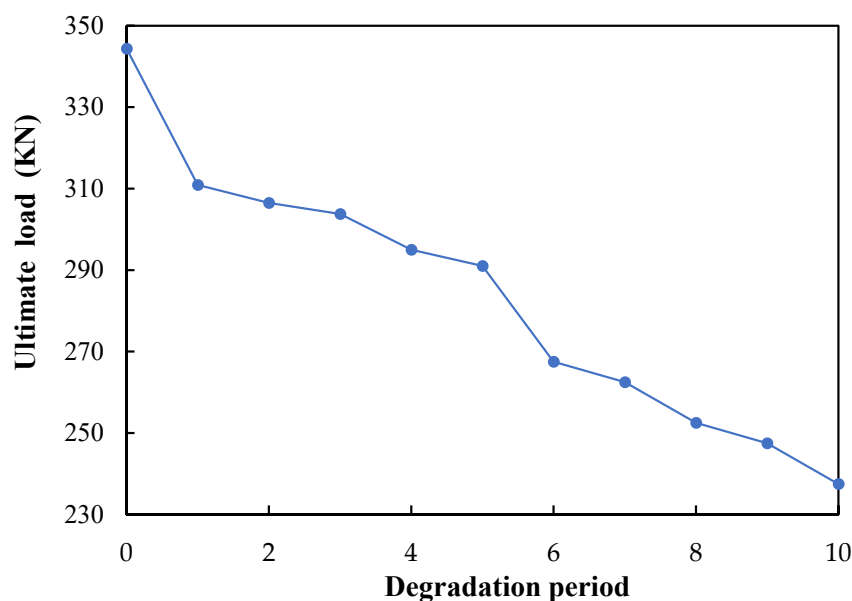


Figure 14. Ultimate loads of degraded reinforced concrete beams in the degradation periods 0–10.

4. Conclusions

This paper studied the degradation of reinforced concrete beams subjected to sustained loading and multi-environmental factors: acid–salt mist, carbon dioxide and the periodic changes of temperature and humidity. In the end of each experimental period, degraded concrete performance and corrode steel bar performance were measured, and degraded reinforced concrete beams were flexurally loaded in four-points bending failure tests. Some conclusions are as follows:

(1) With the deterioration periods increasing, the carbonation depth of degraded concrete increases and more wider cracks are presented on the beam surface. Moreover, the tensile strengths of the corroded longitudinal steel bars declined continuously with the increase in their corrosion rate. As a result of concrete deterioration and steel corrosion, the ultimate loads of degraded reinforced concrete beams subjected to more deterioration periods are obviously lower.

(2) In terms of aggressive factors, the acid–salt mist and carbon dioxide penetrate into reinforced concrete beams and react with concrete and steel bars. The periodic change of temperature and humidity speed up the transmission rate of aggressive factors.

(3) Sustained loading make concrete at bottom of beams loose, which accelerates the degradation of reinforced concrete beams. Compared with individual environmental factor, acid–salt mist, carbon dioxide and the periodic change of temperature and humidity aggravates the degradation of reinforced concrete beams, because the interaction of environmental factors on the beams intensifies the chemical reaction of aggressive factors on concrete or steel bars.

Author Contributions: Conceptualization, H.L.; methodology, H.L. and Z.Z.; validation, Z.Z., J.Y., X.N. and T.H.; formal analysis, S.L.; investigation, S.L.; resources, H.L.; data curation, S.L.; writing—original draft preparation, Z.Z., J.Y. and X.N.; writing—review and editing, S.L.; visualization, S.L.; supervision, H.L.; funding acquisition, S.L. All authors have read and agreed to the published version of the manuscript.

Funding: This research was funded by the Postdoctoral Fund of Jiangsu Collaborative Innovation Center for Building Energy Saving and Construction Technology, grant number SJXTBH02.

Institutional Review Board Statement: Not applicable.

Informed Consent Statement: Not applicable.

Data Availability Statement: The data presented in this study are available on request from the corresponding author.

Conflicts of Interest: The authors declare no conflict of interest.

References

1. Lv, H.L.; Wu, Y.Z.; Fang, Z.N.; Zhou, S.C. Deterioration behavior of reinforced concrete beam under compound effects of acid-salt mist and carbon dioxide. *Construct. Build. Mater.* **2015**, *77*, 253–259. [[CrossRef](#)]
2. Qu, F.L.; Li, W.G.; Dong, W.K.; Tam, V.W.Y.; Yu, T. Durability deterioration of concrete under marine environment from material to structure: A critical review. *J. Build. Eng.* **2021**, *35*, 102074. [[CrossRef](#)]
3. Hossain, K.M.A. Pumice based blended cement concretes exposed to marine environment: Effects of mix composition and curing conditions. *Cement Concr. Compos.* **2008**, *30*, 97–105. [[CrossRef](#)]
4. Yue, P.J.; Tan, Z.Y.; Guo, Z.Y. Microstructure and mechanical properties of recycled aggregate concrete in seawater environment. *Sci. World J.* **2013**, *2013*, 306714. [[CrossRef](#)] [[PubMed](#)]
5. Zhang, Y.; Zhang, M.Z.; Ye, G. Influence of moisture condition on chloride diffusion in partially saturated ordinary Portland cement mortar. *Mater. Struct.* **2018**, *51*, 36. [[CrossRef](#)]
6. Qiao, C.Y.; Ni, W.; Weiss, J. Transport due to diffusion, drying, and wicking in concrete containing a shrinkage-reducing admixture. *J. Mater. Civ. Eng.* **2017**, *29*, 04017146. [[CrossRef](#)]
7. Justnes, H. A review of chloride binding in cementitious systems. *Nord. Concr. Res. Publicat.* **1998**, *21*, 48–63.
8. Bellmann, F.; Möser, B.; Stark, J. Influence of sulfate solution concentration on the formation of gypsum in sulfate resistance test specimen. *Cement Concr. Res.* **2006**, *36*, 358–363. [[CrossRef](#)]
9. Aye, T.; Oguchi, C.T. Resistance of plain and blended cement mortars exposed to severe sulfate attacks. *Construct. Build. Mater.* **2011**, *25*, 2988–2996. [[CrossRef](#)]
10. Guo, L.; Wu, Y.Y.; Xu, F.; Song, X.T.; Ye, J.Y.; Duan, P.; Zhang, Z.H. Sulfate resistance of hybrid fiber reinforced metakaolin geopolymer composites. *Compos. B Eng.* **2020**, *183*, 107689. [[CrossRef](#)]
11. Nehdi, M.; Hayek, M. Behavior of blended cement mortars exposed to sulfate solutions cycling in relative humidity. *Cement Concr. Res.* **2005**, *35*, 731–742. [[CrossRef](#)]
12. Ogawa, S.; Nozaki, T.; Yamada, K.; Hirao, H.; Hooton, R.D. Improvement on sulfate resistance of blended cement with high alumina slag. *Cement Concr. Res.* **2012**, *42*, 244–251. [[CrossRef](#)]
13. Mangat, P.S.; Elgarf, M.S. Flexural strength of concrete beams with corroding reinforcement. *Struct. J.* **1999**, *96*, 149–158.
14. Maaddawy, T.E.I.; Soudki, K.; Topper, T. Long-term performance of corrosion damaged reinforced concrete beams. *ACI Struct. J.* **2005**, *102*, 649–656.
15. Duan, P.; Shui, Z.H.; Chen, W.; Shen, C.H. Influence of metakaolin on pore structure related properties and thermodynamic stability of hydrate phases of concrete in seawater environment. *Construct. Build. Mater.* **2012**, *36*, 947–953. [[CrossRef](#)]
16. Uthaman, S.; Vishwakarma, V.; George, R.P.; Ramachandran, D.; Kumari, K.; Preetha, R.; Premila, M.; Rajaraman, R.; Mudali, U.K.; Amarendra, G. Enhancement of strength and durability of fly ash concrete in seawater environments: Synergistic effect of nanoparticles. *Construct. Build. Mater.* **2018**, *187*, 448–459. [[CrossRef](#)]
17. Jena, T.; Panda, K.C. Compressive strength and carbonation of sea water cured blended concrete. *Int. J. Civ. Eng. Technol.* **2017**, *8*, 153–162.
18. Tsai, W.P.; Chen, H.J.; Pan, H.H.; Hsu, K.C. The accelerated method for estimating corrosion of reinforced concrete structure in seawater. In Proceedings of the 2008 Structures Congress—Structures Congress 2008: Crossing the Borders, Vancouver, BC, Canada, 24–26 April 2008; Volume 314, pp. 1–9.
19. Duan, P.; Zhou, W.; Yan, C. Investigation of pore structure and ITZ of concrete blended with mineral admixtures in a seawater environment. *Mag. Concr. Res.* **2015**, *67*, 812–820. [[CrossRef](#)]
20. Seleem, H.E.-D.H.; Rashad, A.M.; El-Sabbagh, B.A. Durability and strength evaluation of high-performance concrete in marine structures. *Construct. Build. Mater.* **2010**, *24*, 878–884. [[CrossRef](#)]
21. Kondraivendhan, B.; Bhattacharjee, B. Pore size distribution modification of OPC paste through inclusion of fly ash and sand. *Mag. Concr. Res.* **2013**, *65*, 673–684. [[CrossRef](#)]
22. Song, H.W.; Kwon, S.J. Permeability characteristics of carbonated concrete considering capillary pore structure. *Cement Concr. Res.* **2007**, *37*, 909–915. [[CrossRef](#)]
23. Neville, A. Chloride attack of reinforced concrete: An overview. *Mater. Struct.* **1995**, *28*, 63–70. [[CrossRef](#)]
24. Yu, L.W.; François, R.; Dang, V.H.; L’Hostis, V.; Gagné, R. Development of chloride-induced corrosion in pre-cracked RC beams under sustained loading: Effect of load-induced cracks, concrete cover, and exposure conditions. *Cem. Concr. Res.* **2015**, *67*, 246–258. [[CrossRef](#)]
25. Hussain, R.R.; Ishida, T. Influence of connectivity of concrete pores and associated diffusion of oxygen on corrosion of steel under high humidity. *Construct. Build. Mater.* **2010**, *24*, 1014–1019. [[CrossRef](#)]
26. He, S.Q.; Cao, Z.Y.; Liu, W.J.; Shang, F. Experimental study on long-term performance of reinforced concrete beams under a sustained load in a corrosive environment. *Construct. Build. Mater.* **2020**, *234*, 117288. [[CrossRef](#)]

27. Liu, Y.Y.; Fan, Y.F. Experimental study on flexural behavior of prestressed concrete beams reinforced by cfrp under chloride environment. *Adv. Civil Eng.* **2019**, *2019*, 2424518. [[CrossRef](#)]
28. Ramli, M.; Kwan, W.H.; Abas, N.F. Strength and durability of coconut-fiber reinforced concrete in aggressive environments. *Construct. Build. Mater.* **2013**, *38*, 554–566. [[CrossRef](#)]
29. Moreno, J.D.; Pellicer, T.M.; Adam, J.M.; Bonilla, M. Exposure of RC building structures to the marine environment of the Valencia coast. *J. Build. Eng.* **2018**, *15*, 109–121. [[CrossRef](#)]
30. Sawpan, M.A.; Holdsworth, P.G.; Renshaw, P. Glass transitions of hygrothermal aged pultruded glass fibre reinforced polymer rebar by dynamic mechanical thermal analysis. *Mater. Des.* **2012**, *42*, 272–278. [[CrossRef](#)]
31. Marar, K.; Eren, Ö.; Çelik, T. Relationship between impact energy and compression toughness energy of high-strength fiber-reinforced concrete. *Mater. Lett.* **2001**, *47*, 297–304. [[CrossRef](#)]
32. Otieno, M.; Beushausen, H.; Alexander, M. Chloride-induced corrosion of steel in cracked concrete—Part I: Experimental studies under accelerated and natural marine environments. *Cement Concr. Res.* **2016**, *79*, 373–385. [[CrossRef](#)]
33. Darmawan, M.S.; Bayuaji, R.; Sugihardjo, H.; Husin, N.A.; Affandhie, A.; Buyung, R. Shear strength of geopolymer concrete beams using high calcium content fly ash in a marine environment. *Buildings* **2019**, *9*, 98. [[CrossRef](#)]
34. Reddy, D.V.; Edouard, J.B.; Sobhan, K. Durability of fly ash-based geopolymer structural concrete in the marine environment. *J. Mater. Civ. Eng.* **2012**, *25*, 781–787. [[CrossRef](#)]
35. Poupard, O.; Lhostis, V.; Catinaud, S.; Petre-Lazar, I. Corrosion damage diagnosis of a reinforced concrete beam after 40 years natural exposure in marine environment. *Cement Concr. Res.* **2006**, *36*, 504–520. [[CrossRef](#)]
36. Zhu, W.; François, R.; Zhang, C.; Zhang, D. Propagation of corrosion-induced cracks of the RC beam exposed to marine environment under sustained load for a period of 26 years. *Cement Concr. Res.* **2018**, *103*, 66–76. [[CrossRef](#)]
37. Wu, Y.Z.; Lv, H.L.; Zhou, S.C.; Fang, Z.N. Degradation model of bond performance between deteriorated concrete and corroded deformed steel bars. *Construct. Build. Mater.* **2016**, *119*, 89–95. [[CrossRef](#)]